

RELATIVE RADIOMETRIC NORMALIZATION METHODS: OVERVIEW AND AN APPLICATION TO LANDSAT IMAGES

Iosif VOROVENCII, Assoc. prof. PhD. Eng. – Transilvania University of Brasov, Romania, iosif.vorovencii@unitbv.ro

Mihaela Denisa MUNTEAN, PhD. Eng. - Office for Cadastre and Real-Estate Publicity Alba, Romania, mihaela11m@gmail.com

Abstract: *The use of time series of satellite images in different applications requires radiometric corrections. This paper presents five relative radiometric normalization methods (RRN) from the specialized literature and a case study using two Landsat 5 Thematic Mapper (TM) satellite images, acquired in 2007 and 2011. These methods are histogram matching (HM), simple regression (SR), pseudo-invariant features (PIF), dark and bright set (DB), and no-change set determined from scattergrams (NC). The results indicate that, for the studied area, the best methods are HM, SR and NC. The DB and PIF methods fail to produce good results because of the lack of invariant details in the two images, of the high spectral variability specific to agricultural land in the studied area and of the low number of pixels selected to calculate the RRN coefficients.*

Keywords: *RRN, PIF, histogram matching, simple regression.*

1. Introduction

The applications concerning Earth observation involve the use of multitemporal and multisensor satellite images. The main problem in using this type of images is represented by the grey value differences caused by non-surface factors such as sensors, different illumination and atmospheric conditions. These differences make it difficult to compare the images acquired at different dates and under different conditions. In order to reduce the radiometric effects caused by non-surface factors, it is necessary to normalize the images. By applying this pre-processing the grey value differences between temporal images reflect the real changes related to field details.

The radiometric normalization can be performed in two ways, absolutely and relatively. The use of the absolute radiometric normalization is difficult because it involves knowing the conditions which existed at the moment the images were acquired. The absolute normalization methods are based on modeling the physical environment at the moment the image is acquired. Consequently, they require information about the atmospheric absorption and scattering, the visibility and humidity at the moment of acquiring each image in the multitemporal series. The relative radiometric normalization, on the other hand, is widely used in analyzing the land cover/land use changes, the vegetation indices, because it requires no physical data existing at the moment the satellite image was acquired. This method uses a reference image and involves rectifying the others, called subject images, to make them, from a radiometric point of view, equal to or to bring them near the reference image. The specialized literature describes various methods of RRN such as HM, SR, PIF, DB, and NC.

This paper presents the existing methods and employs them to normalize the radiometric difference between two Landsat 5 TM images acquired in 2007 and 2011. The normalized results are compared in terms of visual inspection and statistical analysis.

2. Materials and methods

2.1. Study area

The studied area is located between 44°40'41" and 45°22'48" north latitude and between 26°02'20" and 26°59'24" east longitude. The recorded surface is of 589205 ha and is situated in the south-eastern part of the Curvature Carpathians towards the Romanian Plain (Central Baragan, Gherghitei Plain and Vlasiei Plain) (Figure 1). The area occupies parts of four counties, the western part of Buzau county, the eastern part of Prahova county, the northern part of Ialomita county and the northern part of Ilfov county. Its altitude ranges from 40 m (Baraganul Central Plain) to 750 m (Ciolanul and Istrita Hills).

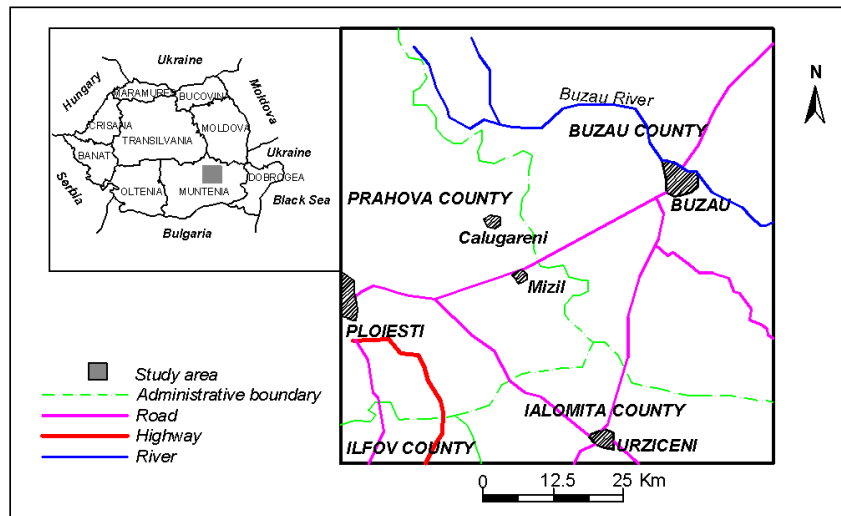


Fig. 1. Study area

The trees are represented by mixtures of deciduous trees (the oak, the Turkey oak, the Hungarian oak, the pedunculate oak and the sessile oak, the hornbeam, the ash tree, the elm tree and the lime tree); at over 500 m beech forest dominate the landscape. The plain area is covered by agricultural land. The soils encountered at altitudes of over 500 m are grey argilluvisols, brown and acid soils. The plain area was formed on soft sediments, dominated at the surface by loessoid formations, alluvia and even sand, and in depth by clays, gravel, sand, sandy marls.

2.2. Materials

The two frames used were clipped from Landsat 5 TM satellite images belonging to path/row 182/29. The images were acquired on 28.07.2007 and 08.08.2011, and have a spatial resolution of 30 m. The 2007 scene represents the subject image and the 2011 one the reference image. The analysis used only the multispectral bands, excluding the thermal one. The images were georeferenced in Universal Transverse Mercator (UTM), zone 35 N, datum WGS 84.

2.3. Methods

Histogram matching is a widely used method of relative radiometric normalization, being integrated in many image processing software packages [6]. This involve first the

equalization of histogram of the subject image in order to obtain an intermediary histogram which is then modified in order to match the reference image histogram. The method normalizes the subject image as compared to the reference image from the point of view of the cumulative density functions of both images using the following formula:

$$DN_N = DF(DN_S) \cdot DF_R^{-1} \quad (1)$$

where: DN_N – the digital value of the pixels in the normalized image; DF – the cumulative density function of the subject image; DN_S – the digital value of the pixels in the subject image; DF_R^{-1} – the reverse cumulative density function of the reference image.

Simple regression involves calculating the normalization coefficients using the entire image, pixel by pixel, observing the following formula [5]:

$$Y_i = a_i X_i + b_i \quad (2)$$

The a_i and b_i coefficients used in the radiometric normalization were determined for each band with the help of the least-square regression method according to the formulas:

$$a_i = \frac{\text{cov}(X_i, Y_i)}{\text{var}(XX)}; \quad b_i = m'_{si} - a_i m'_{ri} \quad (3)$$

where: $\text{cov}(X_i, Y_i)$ – the covariance between the subject and reference images for band (i); $\text{var}(XX)$ – the variance in the subject image for band (i); m'_{si} and m'_{ri} – the average values in the subject and reference images for band (i).

The dark and bright set method is based on the fact that an image contains several pixels presenting details with the same reflectance in the images acquired at different dates [4]. In order to determine the DB set, the greenness-brightness transformation was used, which, for the Landsat 5 TM images, is given by the formulas [1]:

$$\text{Brightness} = 0.2909 (\text{band } 1) + 0.2493 (\text{band } 2) + 0.4806 (\text{band } 3) + 0.5568 (\text{band } 4) + 0.4438 (\text{band } 5) + 0.1706 (\text{band } 7)$$

$$\text{Greenness} = -0.2728 (\text{band } 1) - 0.2174 (\text{band } 2) - 0.5508 (\text{band } 3) + 0.7221 (\text{band } 4) + 0.0733 (\text{band } 5) - 0.1648 (\text{band } 7) \quad (4)$$

Based on them, the dark set and the bright set were determined, using the following formulas:

$$\begin{aligned} \text{Dark set} &= \{ \text{greenness} \leq 1 \text{ and } \text{brightness} \leq 77 \} \\ \text{Bright set} &= \{ \text{greenness} \leq 1 \text{ and } \text{brightness} \geq 180 \} \end{aligned} \quad (5)$$

The normalization coefficients (a_i , b_i) were calculated using the dark set and the bright set obtained for both the subject image and the reference image, by applying the following formulas:

$$a_i = \frac{m_{ri}^b - m_{ri}^d}{m_{si}^b - m_{si}^d}; \quad b_i = m_{ri}^d - a_i \cdot m_{si}^d \quad (6)$$

where: m_{ri}^b – the average value of the bright set (b) in the reference image for band (i); m_{ri}^d – the average value for the dark set (b) in the reference image for band (i); m_{si}^b – the average value of the bright set (b) in the subject image for band (i); m_{si}^d – the average value for the dark set (b) in the subject image for band (i).

Radiometric normalization using PIF was developed by Schott et al. [8] and Salvaggio [7]. The PIF are objects with a reflectance almost invariable from one scene to another acquired on the same area. Generally, these are man-made objects whose reflectance is independent of the season or of biological cycles. The PIF in the case of the Landsat 5 TM images were selected according to the criterion described in the specialized literature based on the intersection of the near infrared and red mask with the infrared threshold mask [2], [11], [9]:

$$\text{PIFset} = \{(\text{band } 4 / \text{band } 3) < 1 \text{ and band } 4 > 180\} \quad (7)$$

The normalization coefficients (a_i , b_i) were obtained on the basis of the PIF selected from the subject and reference images, applying the following formulas:

$$a_i = \frac{s_{ri}}{s_{si}}; \quad b_i = m_{ri} - a_i \cdot m_{si} \quad (8)$$

where: s_{ri} – standard deviation of the PIF set in the reference image for band (i); s_{si} – standard deviation of the PIF set in the subject image for band (i); m_{ri} – the average value in the reference image for band (i); m_{si} – the average value in the subject image for band (i).

No-change set method is based on performing a linear scattergram using the two near infrared bands of the subject and reference images, as well as the two red bands of the same images [2], [10]. In these scattergrams, we identify the water bodies and land centers, which are considered the scattergram portions with the most pixels, and we determine their coordinates. Then, based on them, we calculate the a_i and b_i (a = gain, b = offset) coefficients in order to determine an initial “no-change” axes for band 3 and band 4.

The no-change region is defined on the basis of HPW_{NC} representing the estimated size of the perpendicular marking the half width of the no-change region for band 3 and band 4 scattergrams. The calculations use only the half width HVW_{NC} of the no-change region with the formula:

$$HVW_{NC} = \sqrt{(1 + a_0^2)} \cdot (HPW_{NC}) \quad (9)$$

where a_0 is the slope of the axis initially estimated for a given band. This study of HPW_{NC} relied on the 10 digital numbers value.

The formula for obtaining the NC set is the following:

$$NC = \{(Y_3 - a_{30}X_3 - b_{30}) \leq HVW_{NC_3}\} \text{ and } \{(Y_4 - a_{40}X_4 - b_{40}) \leq HVW_{NC_4}\} \quad (10)$$

where: a_{30} and b_{30} – the initial normalization coefficients for the red band; a_{40} and b_{40} – the initial normalization coefficients for the near infrared band; HVW – the half width of the no-change region; X_3 , X_4 – the digital values in the red and near infrared band of the X subject image; Y_3 , Y_4 – the digital values in the red and near infrared bands of the Y reference image.

After determining the NC, the pixels in this area are used to obtain the normalization coefficients (a_i , b_i) for each band. They are calculated by applying the least square regression method with the following formula:

$$a_i = \frac{\text{cov}(X_i Y_i)}{\text{var}(X_i X_i)}; \quad b_i = m'_{si} - a_i \cdot m'_{ri} \quad (11)$$

where: $\text{cov}(X_i Y_i)$ – the covariance between the subject and reference images for band (i); $\text{var}(X_i X_i)$ – the variance in the subject image for band (i); m'_{si} and m'_{ri} – the averages for the subject and reference images for band (i).

In this study all of the five methods were used. For each of them, the normalization coefficients were calculated for each band and the normalized images were obtained. For each method and band, the study determined the coefficients of variation (CV), the dynamic range (DR), the number of pixels used in calculating the coefficients and the root mean square error (RMSE).

3. Results and discussions

The RRN coefficients obtained after applying the five methods are presented in Table 1. The images obtained after the normalization are represented in Figure 2. The analysed image displayed a large spectral variability as shown by the calculated statistical indicators. The results show that the HM, SR and NC methods allowed us to obtain the most efficient

coefficients for the radiometric normalization. In the case of the DB and PIF methods the gain value (a) is closer to 1.00 and the offset value (b) is almost 0.00 (Table 1). This means that the normalization coefficients calculated and applied to the subject image to match the reference image are less efficient in the studied area. This is also evidenced by the CV and RMSE analysis.

Table 1. The relative normalization coefficients for each band and the RNN

Method	Band 1		Band 2		Band 3		Band 4		Band 5		Band 7	
	a	b	a	b	a	b	a	b	a	b	a	b
HM	-	-	-	-	-	-	-	-	-	-	-	-
SR	0.390	39.389	0.506	13.819	0.443	12.999	0.998	2.045	0.555	26.155	0.510	8.181
DB	1.256	-0.025	1.218	-0.009	1.141	-0.005	1.369	0.000	1.266	0.001	1.166	0.001
PIF	0.670	-0.099	0.695	-0.050	0.679	-0.058	0.664	-0.054	0.591	-0.092	0.565	-0.057
NC	0.826	2.540	0.796	1.645	0.668	3.075	0.947	1.311	0.747	5.209	0.634	3.051

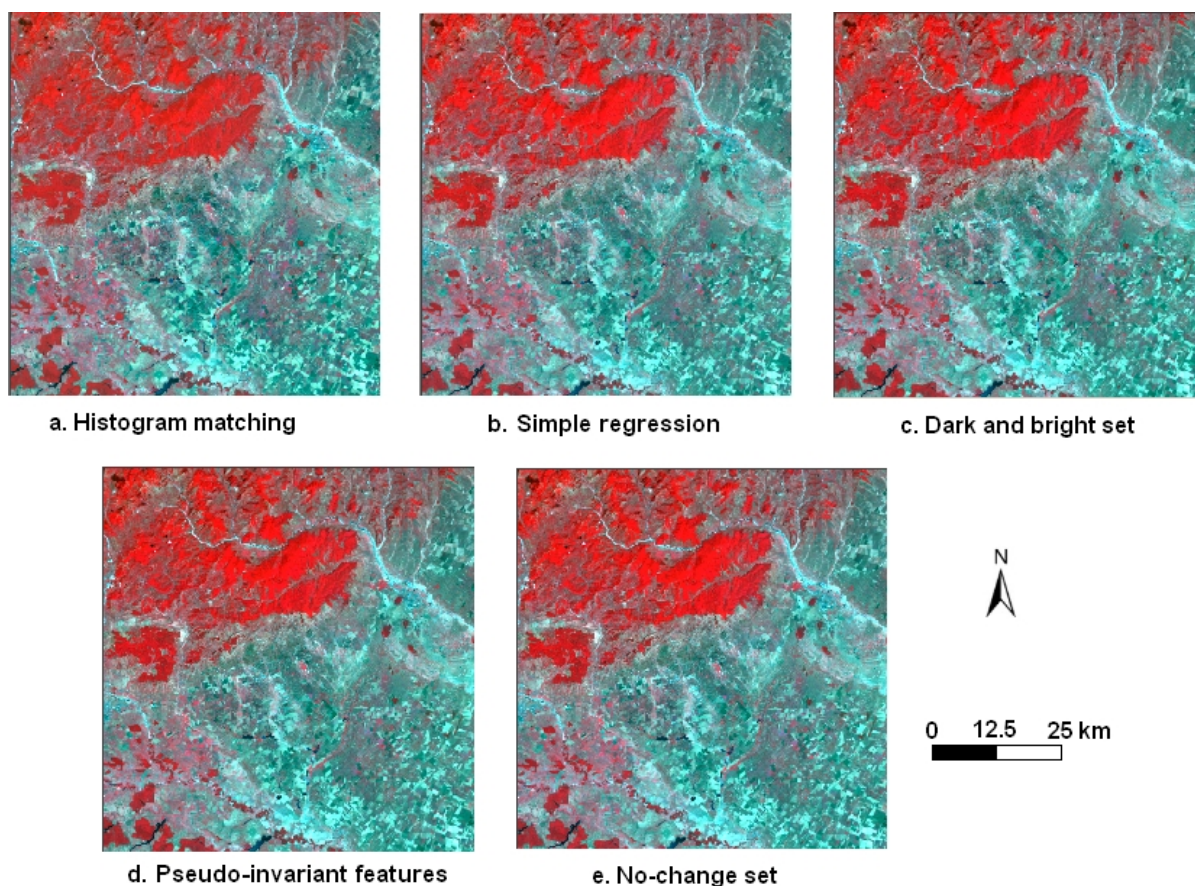


Fig. 2. The 2007 image after relative radiometric normalization

The coefficient of variation does not display for all the RNN methods smaller values compared with CV of raw data (Table 2). Monitoring the values of the variance coefficient, the best radiometric improvement of the subject image was achieved through the SR method, followed by the HM method and the NC method. In the case of the DB and PIF methods CV recorded values slightly elevated than the CV of raw data which means that the two RNN methods failed to improve the radiometric similarity of the subject image to the reference image. The DR displays the same range of values for the HM and DB methods as for the raw data; for the other methods DR has, mostly, lower values than the raw data (Table 2).

Table 2. The coefficient of variation and the dynamic range for each band and RRN

Method	Band 1		Band 2		Band 3		Band 4		Band 5		Band 7	
	CV	DR										
RAW	0.1384	255	0.2633	179	0.3038	255	0.1906	251	0.2241	255	0.3636	255
HM	0.1032	255	0.1578	255	0.2741	255	0.1880	255	0.2129	255	0.3933	255
SR	0.0623	100	0.1124	129	0.1811	113	0.1852	255	0.1575	142	0.2736	130
DB	0.1393	255	0.1889	218	0.3070	255	0.1915	255	0.2248	255	0.3672	255
PIF	0.1393	170	0.1905	124	0.3104	173	0.1919	166	0.2260	150	0.3709	144
NC	0.1345	211	0.1815	143	0.2785	170	0.1889	238	0.2125	190	0.3380	161

The number of pixels taken into consideration when determining the radiometric normalization coefficients represented an important factor. The DB and PIF methods returned the weakest results because of: (1) the low number of pixels taken into consideration in calculating the normalization coefficients (1.97% and 2.87% for the DB method, and 0.44% and 0.21% in the case of the PIF method), and (2) the lack of clear invariant features (Table 3). This shows that most of the details in the studied area changed their spectral nature during the period 2007–2011.

Table 3. Number of pixels considered in RRN

Method	Number of pixels in the subject image		Number of pixels in the reference image		
	Number	%	Number	%	
Raw	6546717	100	6546717	100	
HM	6546717	100	6546717	100	
SR	6546717	100	6546717	100	
DB	Dark	20372	0.31	24580	0.38
	Bright	108792	1.66	163508	2.49
	Total	129164	1.97	188088	2.87
PIF	28796	0.44	13423	0.21	
NC	5304172	81.02	5304172	81.02	

Table 4. The RMSE values obtained after the normalization of the 2007 image

Method	Band 1	Band 2	Band 3	Band 4	Band 5	Band 7	Average
RAW	8.5760	5.3913	9.100	8.0843	23.9032	15.1016	11.6927
HM	2.6762	1.9983	3.2616	7.6263	8.5482	5.2440	4.8924
SR	3.4304	2.3683	3.8690	8.0843	8.3607	5.1755	5.2147
DB	26.1044	12.2864	14.2275	35.0670	49.6963	6.5199	23.9836
PIF	17.9829	6.9331	4.8832	33.9134	22.2146	7.3310	15.5430
NC	5.3057	2.6416	3.4962	9.3286	8.6324	5.1887	5.7655

The RMSE average of raw data is 11.6927; for the HM, SR and NC methods the RMSE averages are lower than the RMSE of raw data which means that these methods were efficient, ensuring the highest accuracy for the relative normalization of the images (Table 4). This is because the fact that the RRN coefficients were calculated taking into consideration all the pixels in the image, that is 81.02% in the case of the NC method. The RMSE for the normalized images obtained through the HM, SR and NC methods are very close for the bands 3, 5 and 7. This means that in these bands the calculated normalization coefficients worked very similarly. Out of the three methods with good results, the NC method allowed the selection of pixels that represent the no-changes area without using all the pixels in the image.

The average RMSE of the DB and PIF methods exceeded the average RMSE of raw data by 105.12%, and 32.93% respectively (Figure 3). Although the threshold value in determining the masks was set by trial, that value proved to be the best and yet the two methods failed to produce good results. This might be mainly because of the high variability within the analysed scene and of the fact that there were no invariant features such as concrete construction, concrete runways etc. Moreover, around 60% of the surface of the studied area represents agricultural land with a high spectral variability in the two images because of different crops in 2007 and 2011. Thus, the obtained results showed that for agricultural land the DB and PIF methods do not return relative normalization coefficients that can improve the radiometry of the image. Also, many of the pixels selected for the DB and PIF methods are pixels that represent river beds which, practically, should not have been included. It was found that they are mistaken for a part of the agricultural land, only a small portion of which was included in the selection. Consequently, the similar spectral behaviour of certain details made them impossible to delimit within the masks used for the two methods.

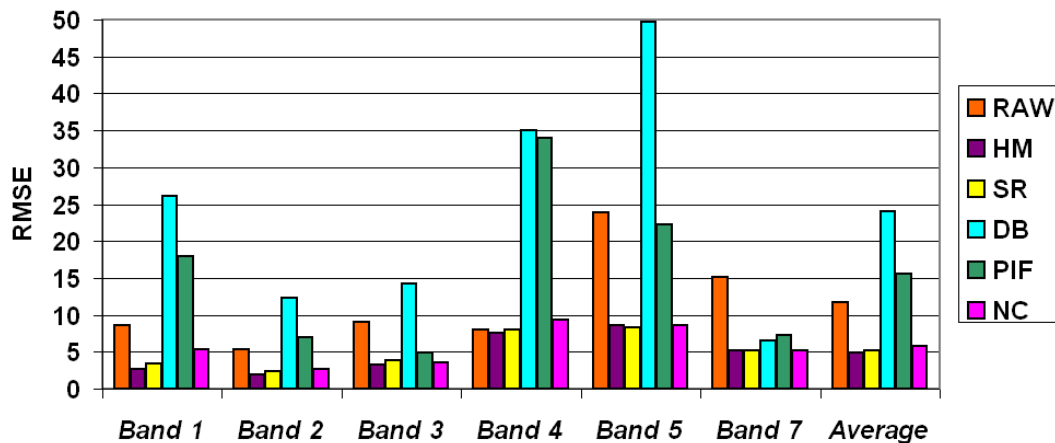


Fig. 3. The RMSE for all bands and all RRN methods

The specialized literature shows also that the use of PIF method in certain areas led to weak results [9]. Other papers, using frames from Quickbird satellite images acquired over the city of Alexandria in Egypt, on an area of 1.728 km², with very many constructions and very few green areas, indicate that the BD and PIF methods produce good results [3]. However, for the area studied in this paper, these methods did not produce good results.

The bands with the highest variability were the infrared ones, i.e. the bands 4 and 5. The highest RMSE values were obtained for these bands in the case of the five RRN methods. In band 4, none of the RRN methods applied produced radiometric normalization coefficients that could lead to lower RMSE. This means that the values for the pixels in band 4 of the 2007 image could not be radiometrically corrected nearer to the values of the pixels in the 2011 image.

4. Conclusions

In this paper, five RRN methods were applied to normalize an image acquired in 2007 after an image acquired in 2011. One of the features of the study performed is the fact that the analysed scene displays a very complex landscape, with an increased spectral variability. The image selected for normalization includes many land cover classes, especially cropland and forests, river beds affected by erosion, water bodies, bare land etc. Within the two images, the percentage of pseudo-invariant features was very small (under 1%). The results show that in

the case of such images the best radiometric normalization coefficients are obtained by applying the HM, SR and NC methods. Whereas, the use of the DB and PIF methods failed to lead to good results, as the RMSE after normalization was even higher than in the raw image. Also, the study revealed that the seasonal variations related to crop rotation in the plain area might represent one of the main reasons that the DB and PIF methods did not produce good results. The results show that, in the case of images with complex landscapes, the methods which took into consideration all the pixels in the image in calculating the RRN coefficients allowed a better normalization of the subject image.

5. References

1. Crist, E. P., Kauth, R. T. – *The Tasseled Cap demystified. Photogrammetric Engineering and Remote Sensing*, 52(1), p. 81-86, 1986.
2. Elvidge, C. D., Yuan, D., Ridgeway, D. W., Lunetta, R.S. – *Relative radiometric normalization of Landsat Multispectral Scanner (MSS) data using an automatic scattergram-controlled regression. Photogrammetric Engineering and Remote Sensing*, 61(10), p. 1255-1260, 1995.
3. Hafify, H. B., El Din, E. H. S. – *Relative radiometric normalization techniques of QuickBird images, Case study: Alexandria City, Egypt. Time Journals of Engineering and Physical Sciences*, 1(2), p. 19-27, 2013.
4. Hall, F. G., Strebel, D. E., Nickeson, J. E., Goetz, S. J. – *Radiometric rectification: Toward a common radiometric response among multitemporal, multisensor images. Remote Sensing of Environment*, 35, p. 11-27, 1991.
5. Jensen, J. R. – *Urban and suburban land use analysis. Manual of Remote Sensing, Second Edition, Vol. II, Interpretation and Applications (John R. Estes, editor), ASPRS, Falls Church, Virginia*, p. 1618-1620, 1983.
6. Richards, J. R. – *Remote Sensing Digital Image Analysis: An Introduction. Springer-Verlag, Berlin*, 281 p, 1986.
7. Salvaggio, C. – *Radiometric scene normalization utilizing statistically invariant features. In: Proceedings of Workshop Atmospheric Correction of Landsat Imagery, Defense Landsat Program Office, Torrance, California*, p. 155-159, 1993.
8. Schott, J. R., Salvaggio, C., Volchok, W. J. – *Radiometric scene normalization using pseudoinvariant features. Remote Sensing of Environment*, 26, p. 1-16, 1988.
9. Yang, X., Lo, C. P. – *Relative radiometric normalization performance for change detection from multi-date satellite images. Photogrammetric Engineering and Remote Sensing*, 66(8), p. 967– 980, 2000.
10. Yuan, D., Elvidge, C. D. – *Application of relative radiometric rectification procedure to Landsat data for use in change detection. In: Proceedings of Workshop Atmospheric Correction of Landsat Imagery. Torrance, California*, p. 162– 166, 1993.
11. Yuan, D., Elvidge, C. D. – *Comparison of relative radiometric normalization techniques. ZSPRS Journal of Remote Sensing*, 51, p. 117-126, 1996.